Investigations into the X and C band Quad-Pol and simulated Compact-Pol features for oil slick characterization

Suman Singha, Maritime Security Lab, German Aerospace Center (DLR), Suman.Singha@dlr.de, Germany
Rudolf Ressel, Maritime Security Lab, German Aerospace Center (DLR), Rudolf.Ressel@dlr.de, Germany
Susanne Lehner, Maritime Security Lab, German Aerospace Center (DLR), Susanne.Lehner@dlr.de, Germany

Abstract

This paper explores the possibilities of quad polarimetric and simulated compact polarimetric SAR data for the purpose of sea ice classification. We propose an array of polarimetric features derived from the Pauli and lexicographic basis scattering matrices, as well as from simulated compact polarimetric data both in C and X band. Those set of features are then used to train and validate an artificial neural network (ANN) based classifier. On a dataset of coincident TerraSAR-X (TS-X) and RADARSAT-2 (RS-2) acquisitions we perform a feature analysis in terms of relevance and redundancy for oil slick characterization .

1 Introduction

Operational detection and discrimination of oil spills over oceans have received considerable attention recently due to its impact on marine ecosystem from environmental and political point of view. Space-borne Synthetic Aperture Radar (SAR) has been used as a major tool for operational oil spill detection activity and attracting significant research interest. [6, 12, 10, 13, 14, 2] One of the major focus regarding oil spill monitoring goes to offshore platform, where operational discharges occurs regularly. As most of the offshore platforms resides in environmentally sensitive zones and also near to costal region (e.g. North Sea and Bombay High platforms clusters) it poses major threat to marine and coastal ecosystem in long term [10, 11]. Until now most of the operational and Near Real Time (NRT) oil spill detection techniques use single-polarization (mainly VV and ground range projected) intensity SAR images where oil spills appear as dark-spots. The sea surface roughness responsible for SAR backscatter is primarily produced by capillary and small gravity waves generated by local winds. Damping of these waves by oil slicks reduces the backscatter, resulting in dark areas in SAR images. Although space-borne SAR system has proven to be a valuable tool for oil spill detection and monitoring, the major challenge still exist, i.e discrimination between oil spill and 'look-alike' spots [13, 7].

2 Dataset

Starting from March 2014 until September 2015, A total number of 20 TerraSAR-X images and 20 RADARSAT-2 images were acquired between March and September 2015 over the study area. Fully polarimetric X-band SAR data have been acquired by TerraSAR-X and TanDEM-X constilation during a scientific exploration campaign started in October 2014 and will continue until December 2015. One of the main objectives of this campaign is to evaluate quad-polarized X-band high resolution SAR data to develop new technologies and applications. X-band quad pol data were acquired using Dual Receive Antenna (DRA) configuration mode. DRA configuration is achieved using electronically splits the long standard antenna (4.8m in Azimuth) during receive into two parts separated in along track ([8], [5]). Therefor, in order to obtain the full scattering matrix the whole antenna is transmitting one polarisation (toggled pulse by pulse to transmit two polarization) and in reception splitting of antenna enables recording of two polarizations ([1]). The X- band fully polarimetric data which were acquired over the study area is quite unique as currently only TerraSAR-X and TanDEM-X constellation is able to provide such space-borne observation (only during science phase).

All of the images acquired, are Single-Look Complex (SSC) product with slant range resolution of approximately 1.2 m in case of TerraSAR-X StripMAP and 5.2 m in case of RADARSAT-2 Fine Quad (FQ) and Fine Quad Wide (FQW) which is ideal for monitoring offshore platform clusters like Bombay High. Figure 1 shows the location of the study area, platform locations and an overview of the acquired TS-X images. The dataset includes different beams of TerraSAR-X StripMAP mode (e.g. StripFar_006, StripNear_009 etc.) and RADARSAT-2 Fine Quad pol Mode (e.g. FQ10, FQ13, FQ6W etc.) incorporating a broad range of incidence angle, from 20 to 35 degree. Incidence angle range was chosen due to it's low instrument noise floor (NESZ range [-19 dB; -26 dB]) which is a critical parameter in respect to the polarimetric system performance. The dataset is strongly heterogeneous, contains several oil spill spots, providing fresh and old platform sourced spills and incorporating different wind conditions. Moreover, the dataset contains a comprehensive set of look-alikes, such as ship wakes and low wind and weather induced dark-spots. A small number of look-alikes present in the data are not from the study area. Figure 2 and 3 show examples of platform sourced oil spill on a RADARSAT-2 Quad polarimetric image acquired on 02nd of June 2015 at 13:16 UTC and on a TS-X StripMAP Quad Pol acquired on 01st of June 2015 at 01:15 UTC respectively over the study area.

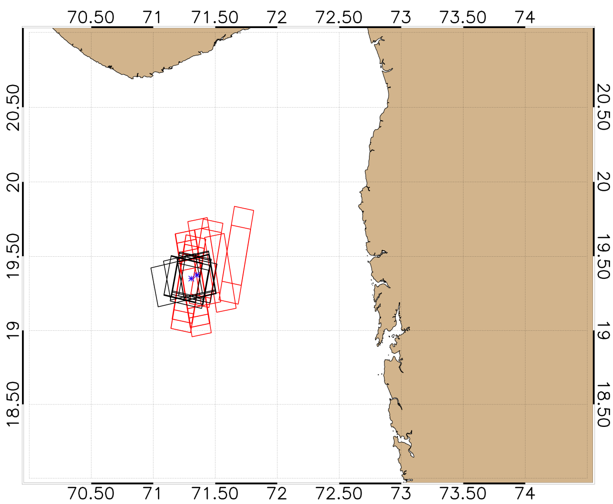

Figure 1: Overview of TerraSAR-X QuadPol StripMap (shown in red) and RADARSAT-2 Fine QuadPol (shown in black) images acquired over Bombay High offshore platform cluster (approximate location of platforms shown in blue marks).

3 Feature analysis

From the resulting scattering matrix S_3 we derive a number of features (e.g., Scattering Diversity, geometric intensity, surface scattering fraction, correlation, real part of the co-pol cross product) which rely on the works of [9].
From the Pauli scattering matrix T_3, we derive the classical $H/A/\alpha$ features (see [3]). Keeping in mind that in future one will also be able to obtain compact polarimetric data from SAR missions (RADARSAT RCM), we also investigate different compact polarimetric features . In order to assess feature quality also for such data, we simulate compact polarimetric data from the full-polarimetric dataset. In particular we generate the $\pi/4$ compact polarimetric scattering matrix from $k_{\pi/4} = 1/\sqrt{2}(S_{HH}+S_{HV}, S_{VV}+S_{VH})$ and the CTLR compact polarimetric (CP) scattering matrices from $k_{CTLR} = 1/\sqrt{2}(S_{HH} - iS_{HV}, -iS_{VV} + S_{VH})$ in order to derive a number of CP features (see Table 1 in [4]), e.g. Stokes vector components, m-χ decomposition features, m-δ decomposition features).
When investigating the quality of the features with respect to classification, we employ the concept of mutual information to assess the relevance of each feature for oil type discrimination and possible redundancies between the different features. One key finding, for which we can also present an underlying analytical explanation, is the possible dispensability of Pauli based features when using certain lexicographic basis features instead. A detailed feature analysis results will be presented in the final paper.

4 Classification results

After pruning the dataset based on the results in the previous step (feature quality analysis), we then use the selected feature set to train and validate an artificial neural network classifier (ANN) based classifier. It is important to note that the training and validation datasets are mutually exclusive. We train the classifier to classify each images in foour different classes: Crude Oil (high density), Emulsion (medium to low density/ weathering effect), Look-Alike and Clear Water. Initially samples from four mentioned classes are gathered from training dataset followed by a standard back-propagation training. The trained classifier are then used to classify images from validation dataset (see Fig 2, 3). Interchanging roles of training set and validation dataset, we were able to find that the classification procedure is stable in terms of the choice of the training data. Despite noticeable biases of the sensors and incidence angle ranges towards certain oil types, the visual comparison of results from C and X band near-coincident acquisitions shows similar oil types (Fig 2, 3). A detailed analysis of results along with analysis of look-alike examples will be presented in final paper.

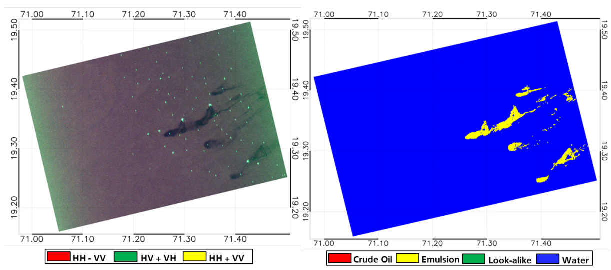

Figure 2: Left: RADARSAT-2 Quad polarimetric image represented in Pauli RGB (Mid incidence angle: $\theta = 25.50°$, Beam Mode: FQ6W) acquired on 02nd of June 2015 at 13:16 UTC (Ascending Orbit) over Bombay High offshore platform cluster (© MDA, 2015). Right: Classification Result.

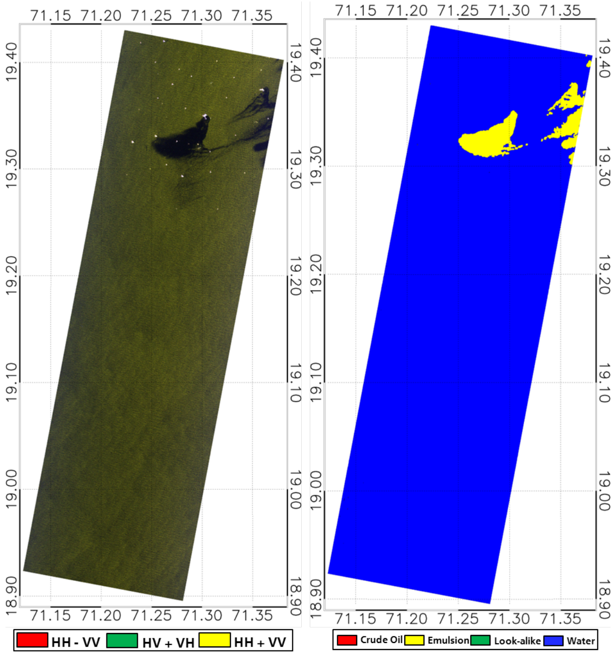

Figure 3: Left: TerraSAR-X Quad polarimetric (mid incidence angle $\theta = 29.63°$) StripMAP (stripFar_006) image acquired on 01st of June 2015 at 01:15 UTC (Descending Orbit) over Bombay High offshore platform cluster (© DLR,2015). Right: Classification Result.

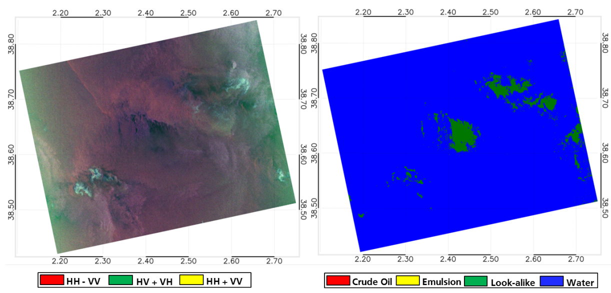

Figure 4: Left: RADARSAT-2 Quad polarimetric image represented in Pauli RGB (Mid incidence angle: $\theta = 29.50°$, Beam Mode: FQ10W) acquired on 30 of November 2012 at 17:42 UTC (Ascending Orbit) over Belearic Sea, south east of Spanish coast (© MDA, 2015). Right: Classification Result.

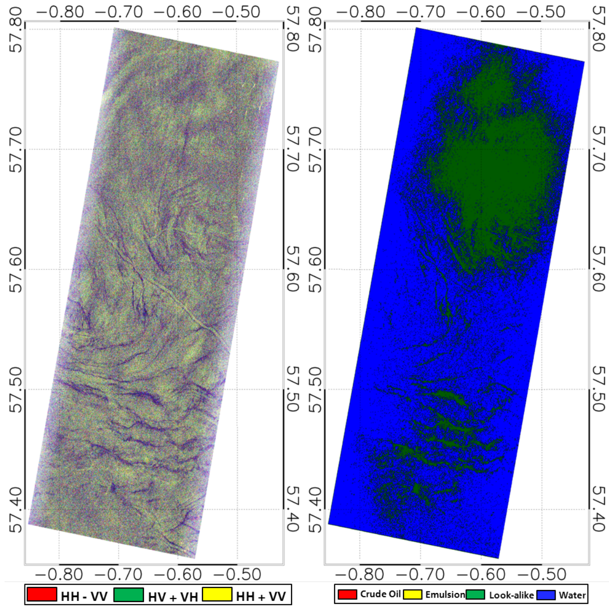

Figure 5: Left: TerraSAR-X Quad polarimetric (mid incidence angle $\theta = 38.80°$) StripMAP (stripNear_011, Contrast enhanced) image acquired on 13th of July 2015 at 06:24 UTC (Descending Orbit) over NorthSea (© DLR,2015). Right: Classification Result.

5 Conclusion

We analyzed the suitability of full-polarimetric and simulated compact polarimetric features in X-band and C-band SAR imagery. We employed to pairs of spatially and temporally correlated acquisitions from TS-X and RS-2 in order to evaluate suitable polarimetric features for oil spill detection. We found in particular that, for the purpose of oil slick characterization, Pauli features can possibly be discarded when including a certain array of S_3 based features. These findings were true both for the TS-X and the RS-2 data. The results show a reasonable visual match between the TS-X and the RS-2 images.

6 Acknowledgment

TerraSAR-X/TanDEM-X Quad Pol Images were acquired through TanDEM-X Science AO: NTI_POLI6690 (PI: Suman Singha) and RADARSAT-2 images were acquired through ESA Category-1 Project Id. C1F.16331 (PI: Susanne Lehner and Suman Singha). RADARSAT-2 Data and Products © MacDonald, Dettwiler and Associates Ltd. (2015) - All Rights Reserved. RADARSAT is an official trademark of the Canadian Space Agency. The views, opinions, and findings contained in this paper are those of the authors and should not be construed as an official DLR position, policy, or decision. The authors would like to thank the TerraSAR-X/TanDEM-X Science Coordination Team for their continuous help regarding acquisitions of TerraSAR-X/TanDEM-X Quad polarization data.

References

[1] H. Breit, T. Fritz, U. Balss, M. Lachaise, A. Niedermeier, and M. Vonavka. Terrasar-x sar processing and products. *Geoscience and Remote Sensing, IEEE Transactions on*, 48(2):727–740, Feb 2010.

[2] Camilla Brekke and Anne H.S. Solberg. Oil spill detection by satellite remote sensing. *Remote Sensing of Environment*, 95(1):1 – 13, 2005.

[3] Shane R Cloude and Eric Pottier. A review of target decomposition theorems in radar polarimetry. *Geoscience and Remote Sensing, IEEE Transactions on*, 34(2):498–518, 1996.

[4] M. Dabboor and T. Geldsetzer. Towards sea ice classification using simulated {RADARSAT} constellation mission compact polarimetric {SAR} imagery. *Remote Sensing of Environment*, 140:189 – 195, 2014.

[5] M. Eineder and T. Fritz. Terrasar-x ground segment experimental product description. Technical Report TX-GS-DD-3303, Issue. 1.3, German Aerospace Center (DLR), 10 2006.

[6] Merv Fingas and Carl Brown. Review of oil spill remote sensing. *Marine Pollution Bulletin*, 83(1):9 – 23, 2014.

[7] Peng Liu, Xiaofeng Li, John J Qu, Wenguang Wang, Chaofang Zhao, and William Pichel. Oil spill detection with fully polarimetric UAVSAR data. *Marine Pollution Bulletin*, 62(12):2611–2618, 2011.

[8] J. Mittermayer and H. Runge. Conceptual studies for exploiting the terrasar-x dual receive antenna. In *Geoscience and Remote Sensing Symposium, 2003. IGARSS '03. Proceedings. 2003 IEEE International*, volume 3, pages 2140–2142, July 2003.

[9] J. Praks, E.C. Koeniguer, and M.T. Hallikainen. Alternatives to Target Entropy and Alpha Angle in SAR Polarimetry. *Geoscience and Remote Sensing, IEEE Transactions on*, 47(7):2262–2274, July 2009.

[10] Suman Singha, Domenico Velotto, and Susanne Lehner. Near real time monitoring of platform sourced pollution using TerraSAR-X over the North Sea. *Marine pollution bulletin*, 86(1):379–390, 2014.

[11] Suman Singha, Domenico Velotto, and Susanne Lehner. Towards Operational Near Real Time Oil Spill Detection Service using Polarimetric TerraSAR-X Image. In *Proceedings of PolInSAR 2015, ESA SP-729*. ESA, 2015.

[12] Suman Singha, Michele Vespe, and Olaf Trieschmann. Automatic Synthetic Aperture Radar based oil spill detection and performance estimation via a semi-automatic operational service benchmark. *Marine Pollution Bulletin*, 73(1):199–209, August 2013.

[13] Anne H Schistad Solberg. Remote sensing of ocean oil-spill pollution. *Proceedings of the IEEE*, 100(10):2931–2945, 2012.

[14] Konstantinos N Topouzelis. Oil spill detection by SAR images: dark formation detection, feature extraction and classification algorithms. *Sensors*, 8(10):6642–6659, 2008.